The intermediate-activity ^{L597V}BRAF mutant acts as an epistatic modifier of oncogenic RAS by enhancing signaling through the RAF/MEK/ERK pathway

Catherine Andreadi,[1] Lai-Kay Cheung,[1] Susan Giblett,[1] Bipin Patel,[1] Hong Jin,[1] Kathryn Mercer,[1] Tamihiro Kamata,[1] Pearl Lee,[1] Alexander Williams,[2] Martin McMahon,[3] Richard Marais,[4,5] and Catrin Pritchard[1,6]

[1]Department of Biochemistry, University of Leicester, Leicester LE1 9HN, United Kingdom; [2]Bioinformatics Core, Gladstone Institute, University of California at San Francisco, San Francisco, California 94158, USA; [3]Helen Diller Family Comprehensive Cancer Center, Department of Cell and Molecular Pharmacology, University of California at San Francisco, San Francisco, California 94143, USA; [4]Signal Transduction Team, The Institute of Cancer Research, Cancer Research UK Centre of Cell and Molecular Biology, London SW3 6JB, United Kingdom

^{L597V}*BRAF* mutations are acquired somatically in human cancer samples and are frequently coincident with *RAS* mutations. Germline ^{L597V}*BRAF* mutations are also found in several autosomal dominant developmental conditions known as RASopathies, raising the important question of how the same mutation can contribute to both pathologies. Using a conditional knock-in mouse model, we show that endogenous expression of ^{L597V}Braf leads to approximately twofold elevated Braf kinase activity and weak activation of the Mek/Erk pathway. This is associated with induction of RASopathy hallmarks including cardiac abnormalities and facial dysmorphia but is not sufficient for tumor formation. We combined ^{L597V}Braf with ^{G12D}Kras and found that ^{L597V}Braf modified ^{G12D}Kras oncogenesis such that fibroblast transformation and lung tumor development were more reminiscent of that driven by the high-activity ^{V600E}Braf mutant. Mek/Erk activation levels were comparable with those driven by ^{V600E}Braf in the double-mutant cells, and the gene expression signature was more similar to that induced by ^{V600E}Braf than ^{G12D}Kras. However, unlike ^{V600E}Braf, Mek/Erk pathway activation was mediated by both Craf and Braf, and ATP-competitive RAF inhibitors induced paradoxical Mek/Erk pathway activation. Our data show that weak activation of the Mek/Erk pathway underpins RASopathies, but in cancer, ^{L597V}Braf epistatically modifies the transforming effects of driver oncogenes.

[*Keywords*: ERK signaling pathway; RASopathies; cancer; oncogene; BRAF]

Supplemental material is available for this article.

Received April 3, 2012; revised version accepted July 18, 2012.

The RAS/RAF/MEK/ERK signaling pathway is a critical mediator of cell growth signals in multiple organisms and cell types. Dysregulation of this pathway is a key characteristic of tumor cells, and components of the pathway are mutational targets in human cancer (Pearson et al. 2001; Davies et al. 2002; Malumbres and Barbacid 2003). In particular, oncogenic *BRAF* and *RAS* mutations are detected in ~7% and ~30% of samples, respectively, and their common ability to activate the downstream MEK/ERK pathway is thought to account at least in part for the transforming effects of these oncogenes (Davies et al. 2002; Malumbres and Barbacid 2003). Germline mutations in components of the RAS/RAF/MEK/ERK pathway, including *BRAF* and *RAS*, are also detected in a group of newly described developmental disorders collectively known as "RASopathies" (Tidyman and Rauen 2009; Rauen et al. 2011). RASopathies include Noonan syndrome (NS), LEOPARD syndrome (LS), Neurofibromatosis type 1 (NF1), Costello syndrome (CS), and cardio–facio–cutaneous syndrome (CFC) and have many overlapping features, including craniofacial abnormalities, cardiac malfunctions, and cutaneous, muscular, and ocular impairments with some increased risk of cancer (Tidyman and Rauen 2009; Rauen et al. 2011).

Of the *BRAF* mutations detected in human cancer, the high-activity ^{V600E}*BRAF* mutation is by far the most

[5]Present address: The Paterson Institute for Cancer Research, The University of Manchester, Wilmslow Road, Manchester M20 4BX, UK.
[6]Corresponding author
E-mail cap8@le.ac.uk
Article published online ahead of print. Article and publication date are online at http://www.genesdev.org/cgi/doi/10.1101/gad.193458.112.

common, being detected in >90% of cases (Davies et al. 2002). However, several other mutations are detected at a lower frequency and have been categorized into high, intermediate, or impaired depending on the level of kinase activity they possess (Wan et al. 2004). Whereas ^{V600E}*BRAF* mutations are mutually exclusive with *RAS* mutations in human cancer samples, the intermediate- and impaired-activity *BRAF* mutations are significantly coincident with *RAS* or other oncogenic driver mutations (http://www.sanger.ac.uk/genetics/CGP/cosmic), suggesting that they may be cooperating rather than driver mutations. In RASopathies, *BRAF* mutations are detected in ~75% of mutation-positive CFC patients and at lower frequencies in NS and LS patients (Rodriguez-Viciana et al. 2006; Sarkozy et al. 2009). All of the *BRAF* mutations are non-^{V600E}*BRAF*. The majority fall into the high- or intermediate-activity class (Rodriguez-Viciana et al. 2006), with only seven also being found in human cancer samples; namely, G469E, F468S, L485F, F595L, V600G, and K601E in CFC patients (Rodriguez-Viciana et al. 2006; Champion et al. 2011), with the intermediate-activity L597V mutation being detected in both NS and CFC patients (Sarkozy et al. 2009; Pierpont et al. 2010).

How the same mutations can promote developmental abnormalities when constitutively expressed but cancer when acquired somatically is a critical question to address and is likely related to mechanisms of downstream MEK/ERK pathway activation under different contexts. High-activity mutants, such as ^{V600E}BRAF, have activity greater than oncogenic RAS-induced ^{WT}BRAF and are known to induce tumor development through their intrinsic ability to hyperactivate the MEK/ERK pathway (Davies et al. 2002; Karasarides et al. 2004). The situation is more complex with lower-activity BRAF mutants. Although impaired-activity mutants have lower activity than ^{WT}BRAF, they induce ERK activation through the formation of heterodimers with CRAF, leading to its activation (Wan et al. 2004; Kamata et al. 2010). Through analysis of the impaired-activity ^{D594A}Braf mutant in mice, we demonstrated that transactivation of Craf in this context was insufficient to drive tumor development per se (Kamata et al. 2010), although, when coexpressed with oncogenic Ras, a cooperating role in tumor development was revealed (Heidorn et al. 2010). Intermediate-activity mutants have activity in between oncogenic RAS-induced ^{WT}BRAF and ^{WT}BRAF and, following overexpression in COS cells, have been shown to induce MEK/ERK activation but to a lower level than high-activity mutants (Wan et al. 2004). CRAF was also transactivated by these mutants in COS cells, although siRNA depletion studies showed that BRAF but not CRAF was responsible for ERK activation in these situations (Wan et al. 2004). Whether mutants of this class are able to drive tumor development in vivo has not yet been addressed, nor has their role in inducing RASopathy syndromes.

Apart from the MEK/ERK pathway, oncogenic RAS can activate multiple downstream signaling pathways, including the phosphatidylinositol 3-kinase (PI3K)/AKT and RalGDS signaling pathways (Malumbres and Barbacid 2003). Of these various pathways, studies in mice have shown a particular dependency on the MEK/ERK pathway for tumor maintenance driven by oncogenic RAS, despite the fact that this pathway is only weakly activated by the oncogene (Tuveson et al. 2004). In two separate reports, treatment of mice with MEK inhibitors showed significant regression of oncogenic Kras-driven tumors in the lung (Ji et al. 2007; Engelman et al. 2008), although a synergistic effect of combined PI3K inhibition was demonstrated in one of these reports (Engelman et al. 2008). Recent studies using knockout mice have also shown a critical role for the Raf/Mek/Erk pathway in lung tumor initiation downstream from oncogenic Kras (Blasco et al. 2011; Karreth et al. 2011). Elimination of both Erk isoforms or both Mek isoforms completely blocked tumor development. However, while knockout of Craf prevented lung tumor development, Braf knockout had no significant effect, indicating that Braf cannot compensate for the loss of Craf and that oncogenic Kras elicits its oncogenic effects through Craf. Consistent with this, oncogenic RAS has been shown to signal exclusively through CRAF to MEK in melanoma cell lines (Dumaz et al. 2006), and Craf has been shown to be required for tumor initiation and maintenance in the DMBA/TPA skin tumorigenesis model in which tumor development is driven by the acquisition of *ras* mutations (Ehrenreiter et al. 2009).

All of the above data reinforce the rationale for targeting RAS/RAF/MEK/ERK as an anti-cancer strategy, an initiative that has been under way for several years now. Although targeted therapies against RAS have largely failed (Basso et al. 2006), the availability of selective chemical inhibitors against RAF, MEK, and ERK have provided new therapeutic opportunities (Montagut and Settleman 2009). RAF inhibitors have made the most progress in the clinic, with the ATP-competitive inhibitor vemurafenib (PLX4032) showing remarkable efficacy in the treatment of melanomas with the ^{V600E}*BRAF* mutation (Chapman et al. 2011). The drug increased rates of overall and progression-free survival in patients with previously untreated melanoma, although resistance to the drug eventually emerged (Johannessen et al. 2010; Nazarian et al. 2010; Chapman et al. 2011; Su et al. 2012). Despite this extraordinary success, the ability of a given cancer to respond to vemurafenib and other similar RAF inhibitors is dependent on *BRAF* mutation status (Hatzivassiliou et al. 2010; Heidorn et al. 2010; Poulikakos et al. 2010). In melanomas with the ^{V600E}*BRAF* mutation, levels of RAS activation are low, and these drugs bind to BRAF monomers, inhibiting their activity (Hatzivassiliou et al. 2010; Heidorn et al. 2010; Poulikakos et al. 2010). However, in ^{WT}BRAF cells, activated RAS promotes dimerization of members of the RAF family, and vemurafenib has been shown to activate signaling through the MEK/ERK pathway by transactivating CRAF (Hatzivassiliou et al. 2010; Heidorn et al. 2010; Poulikakos et al. 2010). This has been hypothesized to explain why ~18% of patients administered with vemurafenib develop squamous cell carcinoma of the skin or keratoacanthoma, with them arising from vemurafenib-induced MEK/ERK pathway activation in cells that have ^{WT}BRAF but active RAS (Chapman et al. 2011; Su et al. 2012). RAF/

MEK inhibitors also offer huge potential for the treatment of RASopathies, and the suppression of RASopathy symptoms in animal models by MEK inhibitors is highly encouraging in this regard (Schuhmacher et al. 2008; Anastasaki et al. 2009; Sarkozy et al. 2009; Rauen et al. 2011). As with cancers, it will be important to understand the mechanisms underpinning RAS/RAF/MEK/ERK pathway deregulation in individual RASopathy patients as a corollary to the implementation of these novel therapies in the clinic.

We focused our efforts on understanding the contribution of each class of *BRAF* mutation to cancer and RASopathies by creating conditional knock-in mouse models with the view to informing better treatments for patients suffering from these diseases. Here, we generated a conditional knock-in mouse for the intermediate activity mutant ^{L597V}Braf and characterized its physiological effects following endogenous expression. We show that constitutive expression of ^{L597V}Braf induces Braf activity intermediate between ^{WT}BRaf and ^{V600E}Braf and weakly activates the Mek/Erk pathway. However, this is not sufficient to induce mouse embryonic fibroblast (MEF) transformation or tumor development in vivo, although the mice do demonstrate a spectrum of RASopathy hallmarks and have some predisposition to cancer when aged. We addressed cooperation with oncogenic Ras by intercrossing with *Kras$^{LSL-G12D}$* mice (Jackson et al. 2001) and found that ^{L597V}Braf has a modifying effect on ^{G12D}Kras-driven MEF transformation and lung tumor formation such that morphological and molecular features are partially transitioned to those driven by ^{V600E}Braf. However, both Craf and Braf mediate Mek/Erk pathway activation in the ^{L597V}Braf-expressing cells and, as with cells expressing ^{WT}BRAF on a mutant RAS background, RAF inhibitors promote Mek/Erk pathway activity rather than inhibiting it. These observations have important implications for the treatment of RASopathy and cancer patients carrying intermediate-activity *BRAF* mutations.

Results

Generation of ^{L597V}Braf-expressing mice

We used a strategy for the generation of Cre-regulated, conditional knock-in *LSL-Braf^{L597V}* mice (Fig. 1A) similar to that previously reported for *LSL-Braf^{V600E}* (Mercer et al. 2005) and *LSL-Braf^{D594A}* (Mercer et al. 2005; Heidorn et al.

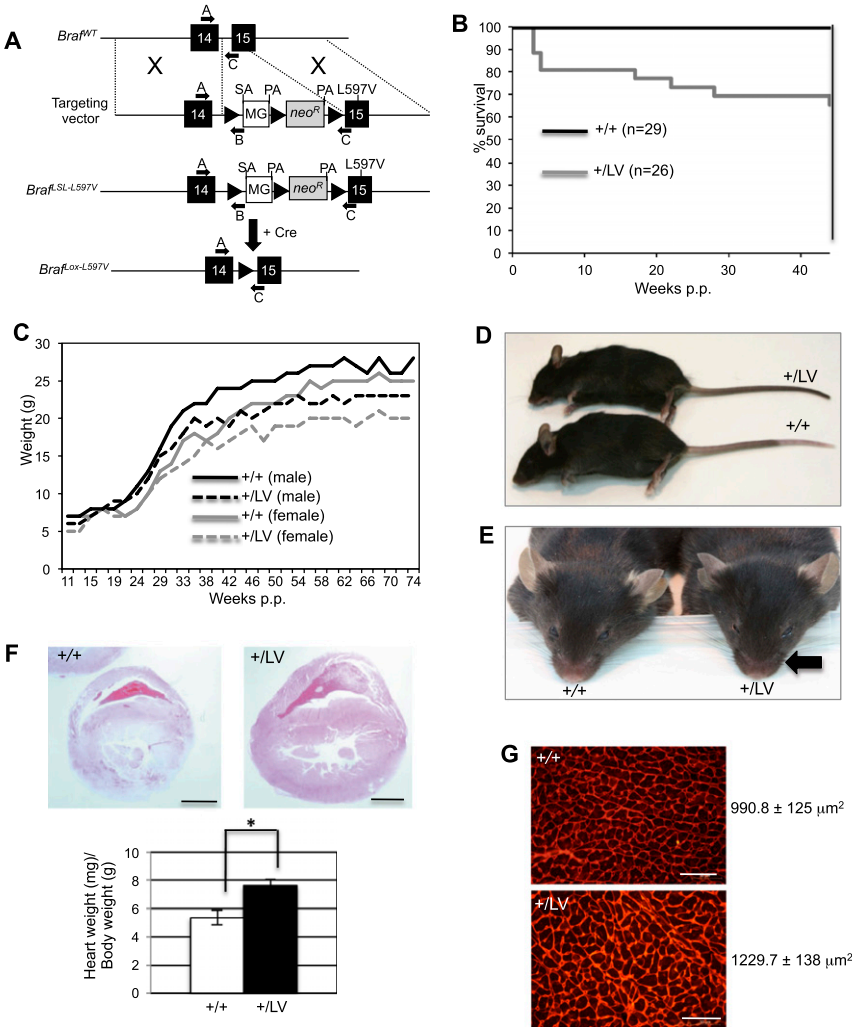

Figure 1. ^{L597V}Braf-expressing mice show RASopathy phenotypes. (*A*) Schematic of the gene-targeting event. The Lox–Stop–Lox (LSL) targeting vector was assembled with mouse *Braf* exon 15 containing the C1789A mutation and minigene *Braf* cDNA exons 15–18 (gray box). Splice acceptor (SA) and polyadenylation (pA) sequences were cloned on either side of the minigene. Cre recombinase induces deletion of the LSL cassette flanked by LoxP sequences (large black arrows), allowing expression of ^{L597V}Braf from the *Braf$^{Lox-L597V}$* allele.(*A–C*) PCR primers to detect wild-type, Lox, and LSL alleles are indicated (small black arrows). (*B*) Survival of littermate *Braf$^{+/+}$* (+/+) and *Braf$^{+/Lox-L597V}$* (+/LV) mice containing the *CMV-Cre* transgene. (*C*) Weight comparisons of littermate +/+ and +/LV mice with the *CMV-Cre* transgene. (*D*) Gross appearance of 3-mo-old +/+ and +/LV female mice. (*E*) Gross facial appearance of 3-mo-old +/+ and +/LV female mice illustrating the blunt nose of mutant animals (arrowhead). (*F*) Enlarged heart. H&E-stained cross-sections of hearts of 3-mo-old mice are shown. Bars, 2 mm. The bar chart indicates the heart weight/body weight ratio of 3-mo-old +/+ ($n = 6$) and +/LV ($n = 3$) mice. (*) $P < 0.01$, Student's *t*-test. (*G*) Wheat germ agglutinin-stained cross-sections of cardiomyocytes. Bars, 100 μm. Cross-sectional areas were measured ($n = 3$ samples per genotype, with 100 cells counted per sample), and the average areas are given *below* for each genotype.

2010; Kamata et al. 2010) mice. Constitutive expression of ^{L597V}Braf from one allele of *Braf* was achieved by intercrossing *Braf*$^{+/LSL\text{-}L597V}$ heterozygous mice with mice heterozygous for the *CMV-Cre* transgene (Schwenk et al. 1995). PCR genotyping was used to confirm inheritance of the *LSL-Braf*^{L597V} allele as well as Cre-mediated recombination to form the *Lox-Braf*^{L597V} allele (Supplemental Fig. S1). On a predominantly C57BL6J background (at least five backcross generations), *Braf*$^{+/Lox\text{-}L597V}$ (+/LV) animals were born alive at the expected Mendelian ratio, but some animals were lost after weaning, with ~70% surviving to adulthood (Fig. 1B).

Mice expressing endogenous ^{L597V}Braf develop RASopathy hallmarks

All surviving +/LV animals were ~10%–20% reduced in weight compared with controls (Fig. 1C). In addition, these animals showed multiple NS/CFC phenotypes, including short stature (Fig. 1D), facial dysmorphia (Fig. 1E), and cardiac enlargement with substantial thickening of the ventricular wall and septum (Fig. 1F). Cardiomyocyte cross-sectional area was increased by ~20% in +/LV mice, indicative of cardiac hypertrophy (Fig. 1G). The surviving +/LV animals developed a spectrum of other pathologies with variable penetrance (Supplemental Table S1). Although they did not develop any signs of advanced cancer, they showed a predisposition to the development of benign tumors, including skin papillomas and intestinal polyps, when aged (Supplemental Fig. S2; Supplemental Table S1).

^{L597V}Braf is a weak activator of the Mek/Erk pathway but does not transform MEFs

To further investigate the transforming potential of ^{L597V}Braf, we induced expression of the mutant protein in MEFs by treating *Braf*$^{+/LSL\text{-}L597V}$ primary MEFs with adenoviral-Cre (AdCre) or adenoviral-βgal (Adβgal). As comparisons, *Braf*$^{+/+}$ and *Braf*$^{+/LSL\text{-}V600E}$ MEFs were simultaneously treated. PCR analysis showed that ~50% recombination of the LSL-L597V and LSL-V600E alleles occurred within 24 h of AdCre treatment, and recombination was virtually complete by 72 h (Supplemental Fig. S3). Previous studies have shown that ^{L597V}BRAF is ~70-fold more active than ^{WT}BRAF, while ^{V600E}BRAF is ~500-fold more active when overexpressed (Wan et al. 2004). To assess the activity of ^{L597V}Braf when endogenously expressed from one allele of *Braf*, as occurs in human cancer, we performed Braf kinase assays of MEF protein lysates. ^{V600E}Braf expression induced approximately eightfold elevated Braf activity, whereas ^{L597V}Braf expression elevated Braf activity by approximately twofold compared with ^{WT}Braf (Fig. 2A). While ^{V600E}Braf expression gave rise to significant induction of phospho-Mek, phospho-Mek was only slightly elevated in LV cells compared with controls (Fig. 2B). However, phospho-Erk reached levels similar to that in VE cells and was not significantly different (Fig. 2B). To explain this paradox, we analyzed the expression of Sprouty2 and Dusp6, negative regulators of the Mek/Erk pathway (Packer et al. 2009; Pratilas et al. 2009), and found that both were significantly induced by ^{V600E}Braf but not by ^{L597V}Braf (Fig. 2B). The induction of Dusp6 could explain, in part, the equivalent levels of phospho-Erk in the VE and LV cells, and indeed, we found that phospho-Erk levels are raised in ^{V600E}Braf cells when the expression of Dusp6 is down-regulated by siRNA knockdown (Supplemental Fig. S4A). As further confirmation of greater Mek/Erk output by ^{V600E}Braf, we also detected higher levels of p90^{RSK} phosphorylation in VE cells compared with LV and wild-type cells (Supplemental Fig. S4B).

Distinct morphological transformation of primary VE MEFs was observed, as previously reported (Mercer et al. 2005), whereas LV MEFs were not transformed and were similar in morphology to control MEFs (Fig. 2C). In addition, VE primary MEFs had an enhanced growth rate (Fig. 2D) and immortalized at early passage number (Fig. 2E), while LV cells had growth and immortalization profiles similar to control MEFs (Fig. 2D,E). Overall, these data show that ^{L597V}Braf is able to induce weakly elevated signaling through the Mek/Erk pathway, and while this is sufficient to induce RASopathy hallmarks, it is not enough to transform primary fibroblasts.

^{L597V}Braf does not induce lung tumor growth in vivo

To examine the cancer phenotype more directly, we focused on the lung, since ^{L597V}*BRAF* mutations are more prevalent in human non-small-cell lung cancer (NSCLC) than any other cancer (http://www.sanger.ac.uk/perl/genetics/CGP/cosmic). The lungs of *Braf*$^{+/Lox\text{-}L597V}$ mice with and without the *CMV-Cre* transgene were examined by H&E staining. In both cases, no histopathological changes were observed compared with controls (Fig. 3A). We also examined the consequences of AdCre delivery to the lungs of *Braf*$^{+/LSL\text{-}L597V}$ mice by nasal inhalation compared with the lungs of *Braf*$^{+/+}$ and *Braf*$^{+/LSL\text{-}V600E}$ mice. While AdCre induced the rapid formation of multiple benign adenomas in the *Braf*$^{+/LSL\text{-}V600E}$ mice (Fig. 3B), as previously reported (Dankort et al. 2007), there were no histopathological changes in the *Braf*$^{+/LSL\text{-}L597V}$ lungs (Fig. 3B). Furthermore, while AdCre delivery gave rise to significant levels of LSL-V600E recombination in the lung, AdCre-mediated LSL-L597V recombination was not detectable (Supplemental Fig. S5A), indicating that ^{L597V}Braf expression in the lung does not give a selective growth advantage.

Constitutive expression of ^{V600E}Braf in mice gives rise to embryonic lethality (Mercer et al. 2005). Therefore, in order to compare Raf–Mek–Erk signaling between the ^{V600E}Braf- and ^{L597V}Braf-expressing lungs, protein lysates were analyzed from the lungs of AdCre-infected *Braf*$^{+/LSL\text{-}V600E}$ mice (Fig. 3B, right panel) in comparison with the lungs of *Braf*$^{+/Lox\text{-}L597V}$;*CMV-Cre*$^{+/o}$ mice (Fig. 3A, middle panel). The *Braf*$^{+/Lox\text{-}L597V}$ lungs had Braf activity in between that of the *Braf*$^{+/+}$ and ^{V600E}Braf-expressing samples (Fig. 3C). Phospho-Mek levels were slightly elevated, but to a significantly lower extent than the ^{V600E}Braf lung,

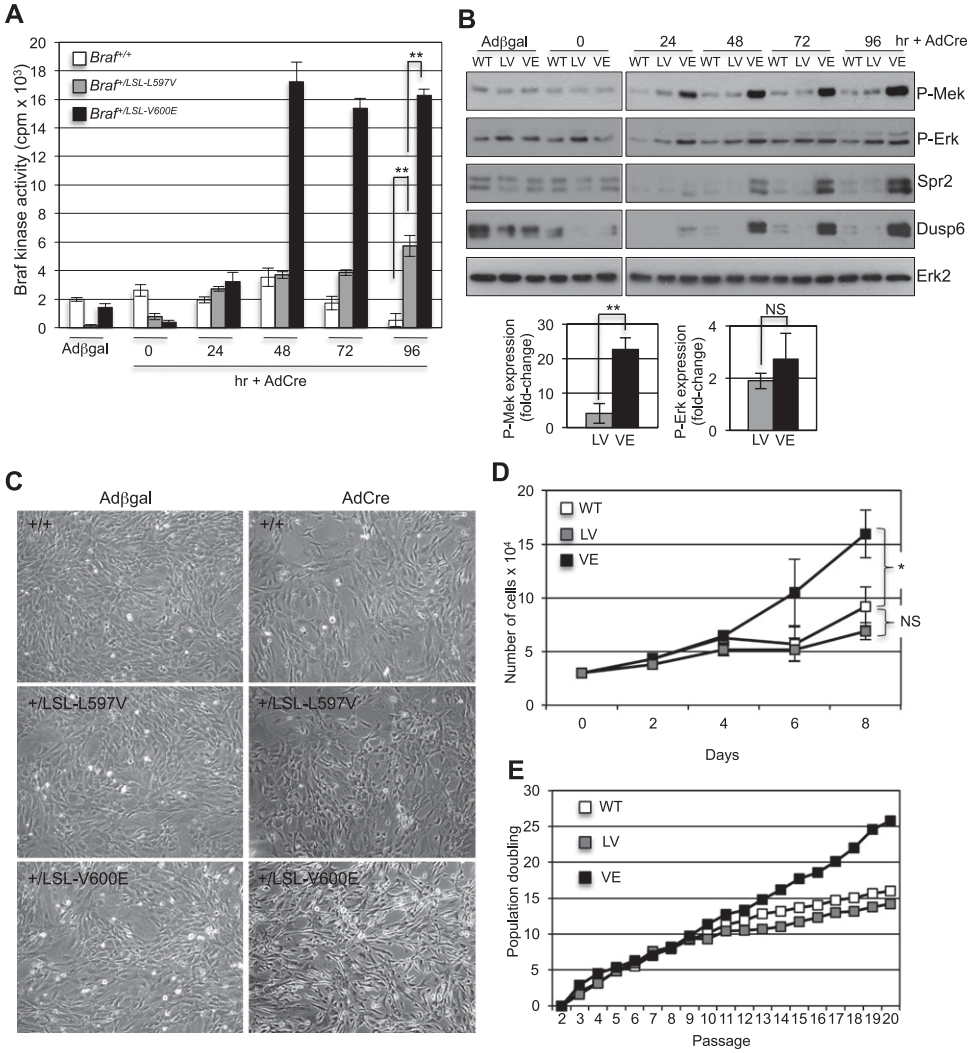

Figure 2. Characterization of MEFs expressing ^{L597V}Braf. (*A*) Braf kinase assays of soluble protein lysates taken from *Braf*$^{+/+}$, *Braf*$^{+/LSL\text{-}L597V}$, and *Braf*$^{+/LSL\text{-}V600E}$ MEFs treated with AdCre for 0–96 h or Adβgal for 96 h. Columns indicate the mean of three samples, and bars indicate the SD. (*B*) Western blot analysis of protein lysates from *Braf*$^{+/+}$, *Braf*$^{+/LSL\text{-}L597V}$, and *Braf*$^{+/LSL\text{-}V600E}$ MEFs treated with AdCre for 0–96 h or Adβgal for 96 h. Western blots were analyzed with the antibodies indicated. Quantification of Western blot analysis of Mek/Erk phosphorylation for the 96-h time point is shown in the graphs *below*. P-Mek and P-Erk levels were normalized to Erk2, the fold changes compared with AdCre-infected wild-type (WT) cells are shown, and error bars indicate the SEM. Data were pooled from three MEFs with the same genotype. (*C*) Representative photographs of *Braf*$^{+/+}$, *Braf*$^{+/LSL\text{-}L597V}$, and *Braf*$^{+/LSL\text{-}V600E}$ MEFs treated with AdCre or Adβgal for 96 h. (*D*) Growth curves of primary *Braf*$^{+/+}$ (wild-type), *Braf*$^{+/Lox\text{-}L597V}$ (LV), and *Braf*$^{+/Lox\text{-}V600E}$ (VE) MEFs over 8 d immediately following 72 h of treatment with AdCre. Mean values of three technical replicates of MEFs of each genotype are shown, and error bars indicate the SEM. These are representative profiles of four different MEFs of each genotype. (*E*) 3T3 immortalization profiles of primary *Braf*$^{+/+}$ (wild-type), *Braf*$^{+/LSL\text{-}L597V}$ (LV), and *Braf*$^{+/LSL\text{-}V600E}$ (VE) MEFs treated with AdCre. Representative profiles of three different MEF lines of each genotypes are shown. For all data, *P*-values were calculated using the Student's *t*-test; (*) $P < 0.01$; (**) $P < 0.005$; (NS) not significant.

whereas phospho-Erk levels were significantly higher in the ^{L597V}Braf lung than the ^{V600E}Braf lung (Fig. 3D), presumably due to the high levels of Dusp6 induced by ^{V600E}Braf (Fig. 3D) that can down-regulate phospho-Erk (Supplemental Fig. S4A). This is a slightly different scenario from MEFs where phospho-Erk levels were comparable in the ^{L597V}Braf and ^{V600E}Braf samples (Fig. 2B), suggesting that there may be tissue-specific differences in regulation of the Mek/Erk pathway. Overall, these data show that, as with MEFs, ^{L597V}Braf has weak activity toward the Mek/Erk pathway in the lung, and this is not sufficient to induce tumor development in vivo.

^{L597V}Braf modifies ^{G12D}Kras-induced MEF transformation

^{L597}BRAF mutations are frequently coincident with other oncogenic driver mutations in human cancer, particularly oncogenic *RAS* mutations (http://www.sanger.ac.uk/perl/genetics/CGP/cosmic). Given that ^{L597V}Braf

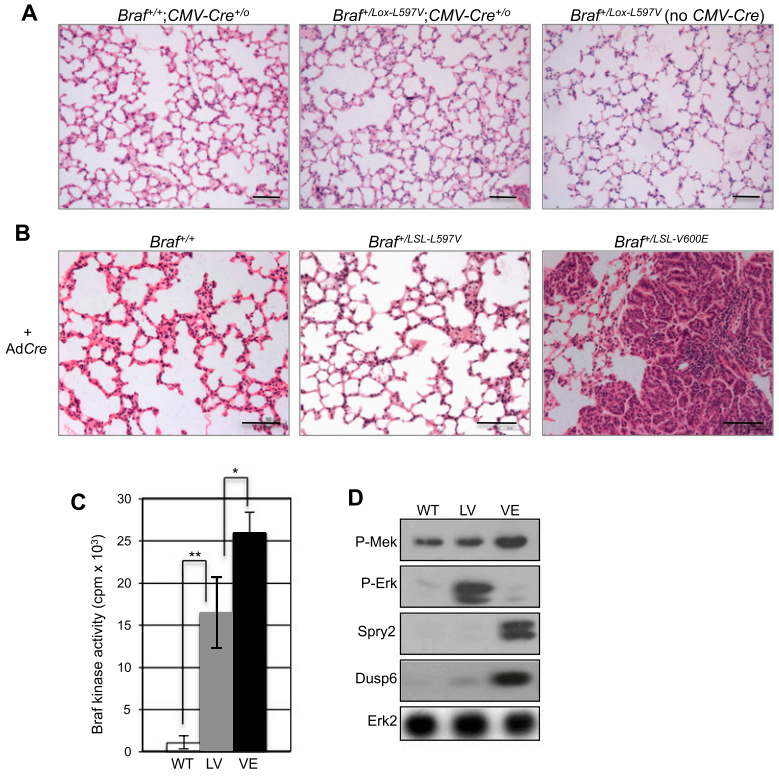

Figure 3. Analysis of ^{L597V}Braf-expressing lung. (*A*) H&E-stained lung sections taken from *Braf*$^{+/+}$;*CMV-Cre*$^{+/o}$ mice, *Braf*$^{+/Lox\text{-}L597V}$;*CMV-Cre*$^{+/o}$ mice, or *Braf*$^{+/Lox\text{-}L597V}$ mice lacking the *CMV-Cre* transgene. Bars, 100 μm. (*B*) H&E-stained lung sections taken from *Braf*$^{+/+}$, *Braf*$^{+/LSL\text{-}L597V}$, and *Braf*$^{+/LSL\text{-}V600E}$ mice treated with 1×10^8 plaque-forming units (pfu) by nasal inhalation 8 wk post-AdCre infection. Bars, 100 μm. (*C*) Braf kinase assays of protein lysates prepared from the lungs of *Braf*$^{+/+}$;*CMV-Cre*$^{+/o}$ (wild-type) and *Braf*$^{+/Lox\text{-}L597V}$;*CMV-Cre*$^{+/o}$ (LV) mice as well as protein lysates prepared from *Braf*$^{+/LSL\text{-}V600E}$ mice treated with 1×10^8 pfu of AdCre by nasal inhalation 8 wk post-AdCre infection (VE). Columns indicate the mean of three technical replicates of three different biological samples, and bars indicate the SD. *P*-values were calculated using the Student's *t*-test; (**) $P < 0.005$; (*) $P < 0.01$. (*D*) Western blot analysis of protein lysates prepared from the lungs of *Braf*$^{+/+}$;*CMV-Cre*$^{+/o}$ (wild-type), *Braf*$^{+/Lox\text{-}L597V}$;*CMV-Cre*$^{+/o}$ (LV), and *Braf*$^{+/LSL\text{-}V600E}$ mice treated with 1×10^8 pfu of AdCre by nasal inhalation 8 wk post-AdCre infection (VE). Western blots were analyzed with the antibodies indicated.

is not able to transform cells on its own (Fig. 2C), we assessed its role in modifying ^{G12D}Kras transformation. *Braf*$^{+/LSL\text{-}L597V}$ mice were intercrossed with *Kras*$^{+/LSL\text{-}G12D}$ mice (Jackson et al. 2001), and double heterozygotes were obtained along with single heterozygote controls. Primary MEFs were treated with AdCre along with *Braf*$^{+/LSL\text{-}V600E}$ MEFs, and Cre-mediated recombination of Lox–Stop–Lox (LSL) alleles was confirmed by PCR genotyping (Supplemental Fig. S5B). Consistent with previous observations (Tuveson et al. 2004; Mercer et al. 2005), G12D and VE MEFs showed evidence of transformation, although the ^{V600E}Braf-driven morphology was far more distinct than that driven by ^{G12D}Kras (Fig. 4A). Adding *^{L597V}Braf* and *^{G12D}Kras* mutations together led to a more striking morphological transformation than either mutation alone, and the double-mutant cells were more similar to VE cells in this regard (Fig. 4A).

The *^{G12D}Kras* and *^{L597V}Braf* mutations together induced significantly higher levels of phospho-Mek than either mutation alone (Fig. 4B,C). Phospho-Erk levels were not significantly different between the single- and double-mutant cells, presumably because of alterations in the expression of Dusps (Fig. 4B,C). Indeed, the double-mutant MEFs had significantly higher Dusp6 levels compared with the single-mutant G12D or LV cells (Fig. 4B,C). Sprouty2 levels were higher in the G12D/LV cells compared with the LV cells but were not significantly different between the G12D/LV and G12D cells (Fig. 4C), suggesting that Sprouty2 expression may also be regulated by non-Mek/Erk pathways in MEFs.

Analysis of the growth of primary cells showed that G12D cells had higher growth rates than VE cells, whereas the double-mutant cells grew in between the two (Fig. 4D). The G12D/LV MEFs underwent early immortalization, although the kinetics of immortalization was delayed in comparison with G12D cells, with them immortalizing at a passage number more similar to the VE cells (Fig. 4E). The slower growth and immortalization of VE and G12D/LV MEFs in comparison with G12D cells may be related to the higher Mek/Erk signaling in these cells and the consequent impact on D-type cyclin expression. Indeed, we found that, although the expression of Cyclin d1 and d2 was elevated in VE, G12D, and G12D/LV cells compared with control and LV cells, Cyclin d3 was only elevated in G12D cells (Supplemental Fig. S6). Overall, these data show that ^{L597V}Braf enhances ^{G12D}Kras signaling through the Mek/Erk pathway, and this has the effect of partially converting ^{G12D}Kras to an oncogene more like ^{V600E}Braf.

^{L597V}Braf modifies ^{G12D}Kras-induced lung tumor development

^{G12D}Kras and ^{V600E}Braf induce the formation of pulmonary preneoplastic lesions with similar histopathological characteristics (Jackson et al. 2001; Dankort et al. 2007), and both are dependent on the Erk signaling pathway for tumor maintenance (Ji et al. 2007). The major difference between the two is that ^{V600E}Braf induces more rapid tumor growth followed by the induction of senescence, whereas ^{G12D}Kras elicits faster progression to adenocarcinoma. We administered AdCre by nasal inhalation to *Kras*$^{+/LSL\text{-}G12D}$ and *Braf*$^{+/LSL\text{-}V600E}$ mice as well as double-mutant *Kras*$^{+/LSL\text{-}G12D}$;*Braf*$^{+/LSL\text{-}L597V}$ mice and analyzed

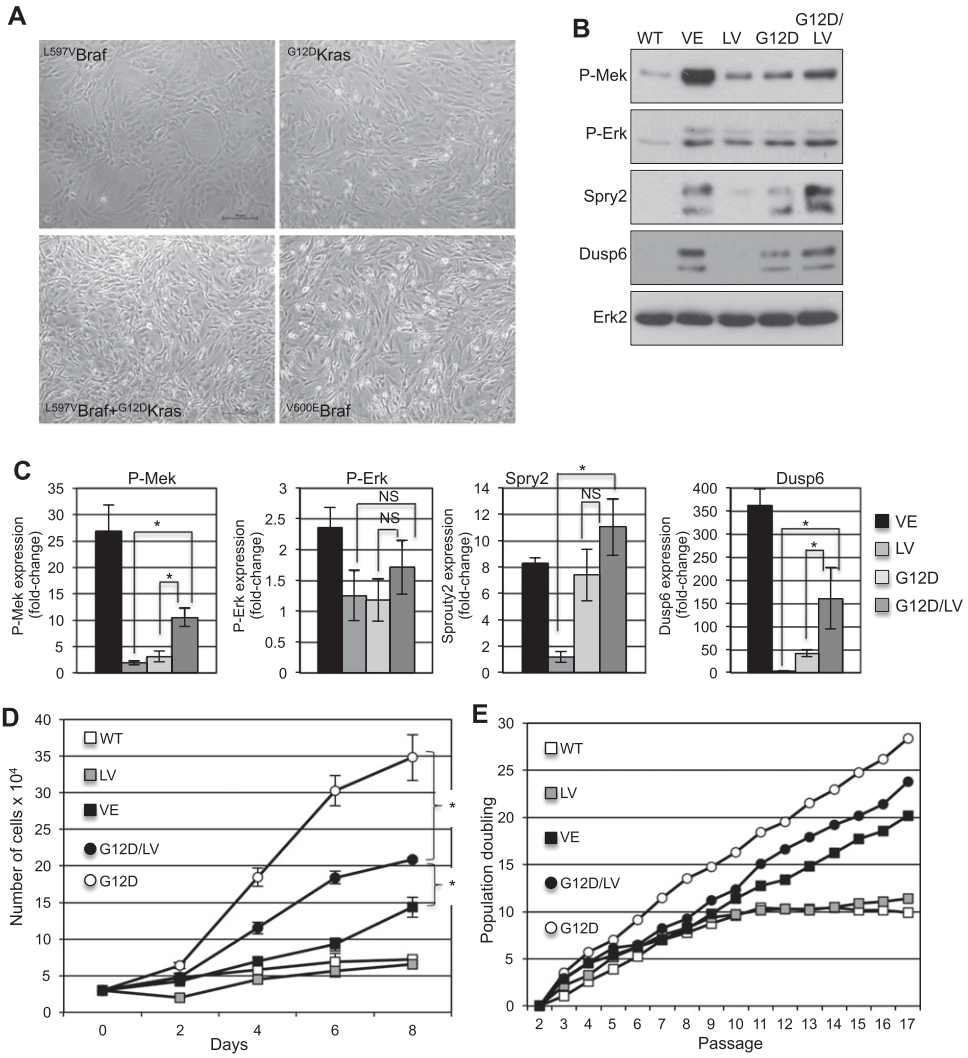

Figure 4. ^{L597V}Braf modifies ^{G12D}Kras MEF transformation. (*A*) Representative photographs of primary MEFs. (*B*) Western blot analysis of protein lysates from primary MEFs. Western blots were analyzed with the antibodies indicated. (*C*) Quantification of Western blot analysis of Mek/Erk phosphorylation and Dusp6/Sprouty2 expression. P-Mek, P-Erk, Dusp6, and Sprouty2 levels were normalized to Erk2, and the fold changes compared with wild-type MEFs are shown, where error bars indicate the SEM. Data were pooled from three MEFs with the same genotype. (*D*) Growth curves of primary MEFs over 8 d immediately following 72 h of treatment with AdCre. Mean values of three technical replicates of MEFs of each genotype are shown, and error bars indicate the SEM. These are representative profiles of four different MEFs of each genotype. (*E*) 3T3 immortalization profiles of MEFs treated with AdCre. Representative profiles of three different MEF lines of each genotype are shown. For all data, *P*-values were calculated using the Student's *t*-test; (*) $P < 0.01$; (NS) not significant.

lung tumor development at 8 and 12 wk post-AdCre treatment. Cre-mediated recombination was confirmed by PCR (Supplemental Fig. S5A). The VE lung had a higher tumor burden than the G12D lung, and the tumor burden for the G12D/LV lung remained similar to that driven by G12D (Fig. 5A,B). Consistent with previous observations (Jackson et al. 2001; Dankort et al. 2007), ^{G12D}Kras and ^{V600E}Braf induced a spectrum of preneoplastic lesions, including bronchiolar hyperplasia (BH), adenomatous alveolar hyperplasia (AAH), and adenomas, although ^{V600E}Braf induced far more adenomas and fewer AAH lesions than ^{G12D}Kras (Fig. 5A,C). The presence of ^{L597V}Braf on top of ^{G12D}Kras generated significantly more adenomas but fewer AAH lesions (Fig. 5A,C). Mosaic Cre-mediated recombination is a more frequent occurrence with multiple floxed alleles, and indeed, a lower level of recombination of the $Braf^{LSL}$ allele was observed in the G12D/LV lung compared with the VE lung (Supplemental Fig. S5A). This may account in part for the observation that the G12D/LV phenotype is only partially transitioned to the VE lung phenotype (Fig. 5A–C). While occasional adenocarcinoma transitions were observed in the G12D mice (two of 10 mice analyzed), none were observed in the VE mice (zero of 10 mice analyzed) or G12D/LV mice (zero of 11 mice analyzed). Activation of the Mek/Erk pathway and the expression of downstream

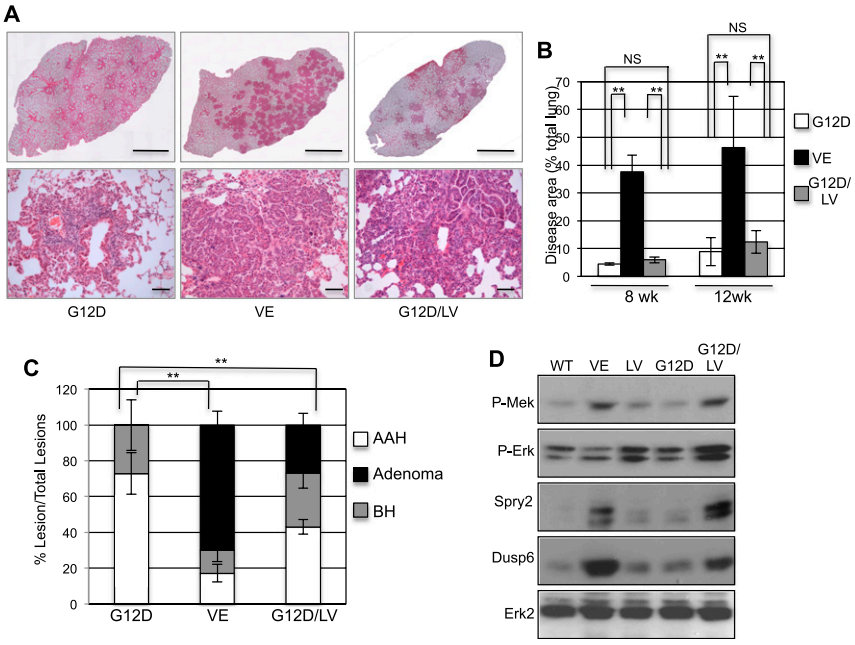

Figure 5. ^{L597V}Braf modifies ^{G12D}Kras-driven lung tumorigenesis. (*A*) H&E staining of representative lung sections from *Kras*$^{+/LSL\text{-}G12D}$, *Braf*$^{+/LSL\text{-}V600E}$, and *Braf*$^{+/LSL\text{-}L597V}$;*Kras*$^{+/LSL\text{-}G12D}$ mice treated with 1×10^8 pfu of AdCre 8 wk post-infection. Bars: *top* panels, 2 mm; *bottom* panels, 100 μm. (*B*) Tumor burden in lungs of *Kras*$^{+/LSL\text{-}G12D}$, *Braf*$^{+/LSL\text{-}V600E}$, and *Braf*$^{+/LSL\text{-}L597V}$;*Kras*$^{+/LSL\text{-}G12D}$ mice at 8 and 12 wk post-infection with 1×10^8 pfu of AdCre. Burden was determined as the percent diseased area per total lung area. Data represent the mean of three samples of each genotype at each time point, and error bars indicate the SD. (*C*) Percent of pulmonary lesions with respect to the total number of lesions in *Kras*$^{+/LSL\text{-}G12D}$, *Braf*$^{+/LSL\text{-}V600E}$, and *Braf*$^{+/LSL\text{-}L597V}$;*Kras*$^{+/LSL\text{-}G12D}$ mice treated with 1×10^8 pfu of AdCre pooled from 8- and 12-wk time points combined. Data represent the mean of six samples of each genotype, and error bars indicate the SD. For *B* and *C*, *P*-values were calculated using the Student's *t*-test; (**) $P < 0.005$; (NS) not significant. (*D*) Western blot analysis of protein lysates from the lungs of *Braf*$^{+/+}$, *Kras*$^{+/LSL\text{-}G12D}$, *Braf*$^{+/Lox\text{-}V600E}$, and *Braf*$^{+/Lox\text{-}L597V}$;*Kras*$^{+/Lox\text{-}G12D}$ mice treated with 1×10^8 pfu of AdCre 8 wk post-infection and lysates from lungs of *Braf*$^{+/LSL\text{-}L597V}$;*CMV-Cre*$^{+/o}$ mice. Western blots were analyzed with the antibodies indicated.

targets Dusp6 and Sprouty2 were enhanced by combining the ^{L597V}Braf mutation with the ^{G12D}Kras mutation (Fig. 5D). Thus, as in MEFs, ^{L597V}Braf modifies ^{G12D}Kras-driven lung tumor development such that there is a partial transition to tumors with biochemical and histological features more similar to those driven by ^{V600E}Braf.

Transcriptome profiling

In order to perform a more direct assessment of the impact of ^{L597V}Braf on ^{G12D}Kras, we undertook microarray comparison of genes expressed in immortalized wild-type, LV, VE, G12D, and G12D/LV MEFs. Following microarray normalization and summarization, analysis of variance (ANOVA) with a 0.01 false discovery rate (FDR) threshold was used to identify genes significantly altered compared with wild-type controls (Supplemental Table S2). For all genotypes, more genes were up-regulated than were down-regulated (Fig. 6A). There were 137 gene changes in the LV samples, 404 in the G12D samples, 492 in the G12D/LV samples, and 975 in the VE samples (Fig. 6B,C). Thus, consistent with the morphology data (Fig. 4A), ^{L597V}Braf had a weaker molecular effect than either of the other mutations, whereas ^{V600E}Braf had the strongest molecular effect. Less than 20% of the gene expression changes observed in the LV MEFs were shared with G12D or VE MEFs, whereas ~50% of the gene changes induced by G12D were shared by VE (223 genes) (Fig. 6A,B). Given that previous studies in melanoma cells have shown that the gene expression signature induced by ^{V600E}BRAF is attributable to signaling through the MEK/ERK pathway (Packer et al. 2009), these data suggest that approximately half of the gene changes induced by ^{G12D}Kras arise through signaling through this pathway, and the weak effect of ^{L597V}Braf on the Mek/Erk pathway is insufficient to induce cognate transcriptional changes.

Of the gene changes observed in the G12D/LV samples, ~40% were also found in single-mutant samples alone, predominantly within the G12D cohort (Fig. 6C,D), indicating that the combination of the two mutations is able to mirror the molecular effects of either mutation alone to some extent, but additional molecular changes are induced on top of this. Indeed, the G12D/LV samples had more gene expression changes shared in common with VE than G12D (~65% compared with 40%) (Fig. 6C,D), suggesting that ^{L597V}Braf may subvert some of the signaling induced by ^{G12D}Kras away from other Ras–effector pathways toward the Mek/Erk pathway. In addition, ~30% of the gene changes in the G12D/LV samples were not shared with either VE or G12D (146 of 492 genes) (Fig. 6D), suggesting that ^{L597V}Braf may act to regulate Mek/Erk-independent and Ras-independent signaling pathways.

Gene ontology analysis performed using GenMAPP (http://www.genmapp.org/go_elite) showed that the gene changes shared by VE, G12D, and G12D/LV (Supplemental Table S3) were enriched for those involved in inactivation of the MAPK pathway, although this was not quite statistically significant ($P = 0.0574$, adjusted for multiple hypothesis testing); presumably, this occurs as a response to hyperactivation of the Mek/Erk pathway in these cells (Fig. 4B). No other enrichments were observed in other data sets except for gene changes unique to G12D/LV that showed a preponderance for genes involved in RNA binding and translation (Supplemental Table S4).

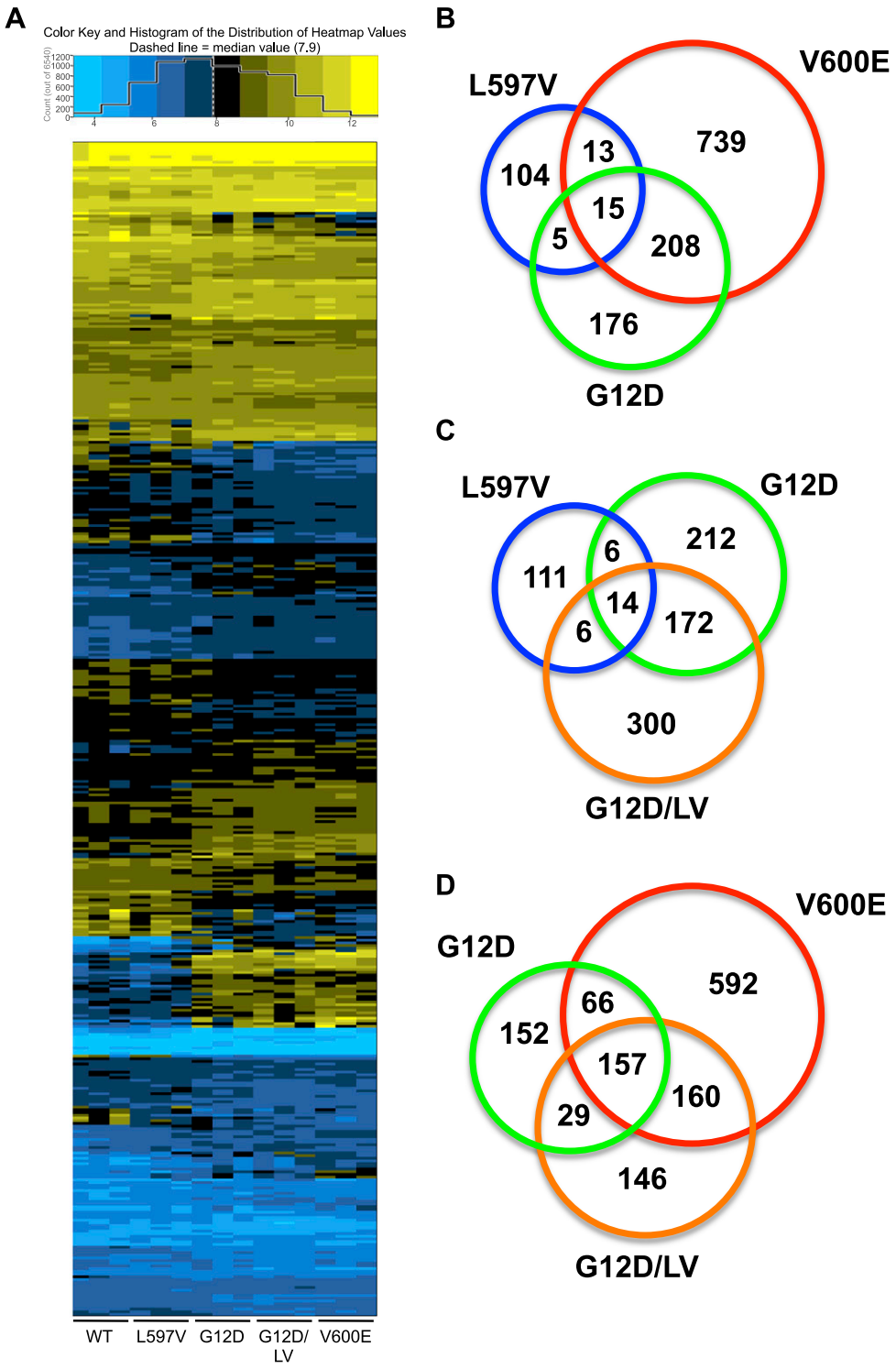

Figure 6. Microarray analysis. (*A*) Heat map of 436 genes significantly differentially expressed in G12D/LV MEFs compared with wild-type MEFs at a cutoff raw *P*-value of <0.01 in each of the biological samples. Values were generated through Affymetrix RMA normalization of all of the arrays, and the expression represents the absolute level of expression. The scale is $\log_2$, and the median expression level for the whole genome is ~7.9. Genes are ordered by magnitude of differential expression. (*B–D*) Venn diagrams indicating numbers of shared genes differentially expressed in each of the samples indicated compared with wild-type samples at a cutoff raw *P*-value of <0.01.

^{L597V}*Braf signals through Braf and Craf*

Impaired-activity BRAF mutants are known to transactivate CRAF (Wan et al. 2004; Kamata et al. 2010). To assess whether this is also the case for intermediate-activity mutants, Craf activity was assessed in LV MEFs and lungs and compared with wild-type as well as VE, G12D, and G12D/LV samples. Craf activity was significantly elevated by ~5.4-fold and ~1.7-fold in the LV lungs and MEFs, respectively, compared with wild-type samples, while Craf activity was not significantly elevated in the VE samples (Fig. 7A,B). The kinase activities of both Braf and Craf were slightly elevated by G12D, but there was striking induction of Craf activity in the G12D/LV lungs and MEFs of ~20-fold and ~8.7-fold, respectively (Fig. 7A,B). *Craf* and *Braf* siRNA was performed on immortalized MEFs to identify the contribution of each isoform to downstream Mek/Erk activation. As previously determined for cells expressing ^{V600E}Braf, siRNA knockdown of *Braf* but not *Craf* significantly suppressed Mek phosphorylation (Fig. 7C). In G12D cells, *Craf* or *Braf* siRNA alone significantly suppressed Mek phosphorylation, although there was a greater suppression following combined Braf/Craf siRNA knockdown (Fig. 7C). The LV and G12D/LV cells responded in a way similar to the G12D cells. In several cases, alterations in phospho-Erk levels did not always correlate with phospho-Mek levels; this is likely attributable to changes in expression of Dusps arising as a result of Braf/Craf down-regulation.

RAF inhibitors induce paradoxical Mek/Erk activation

Small molecule inhibitors targeting BRAF are now in clinical use as anti-cancer therapies (Chapman et al.

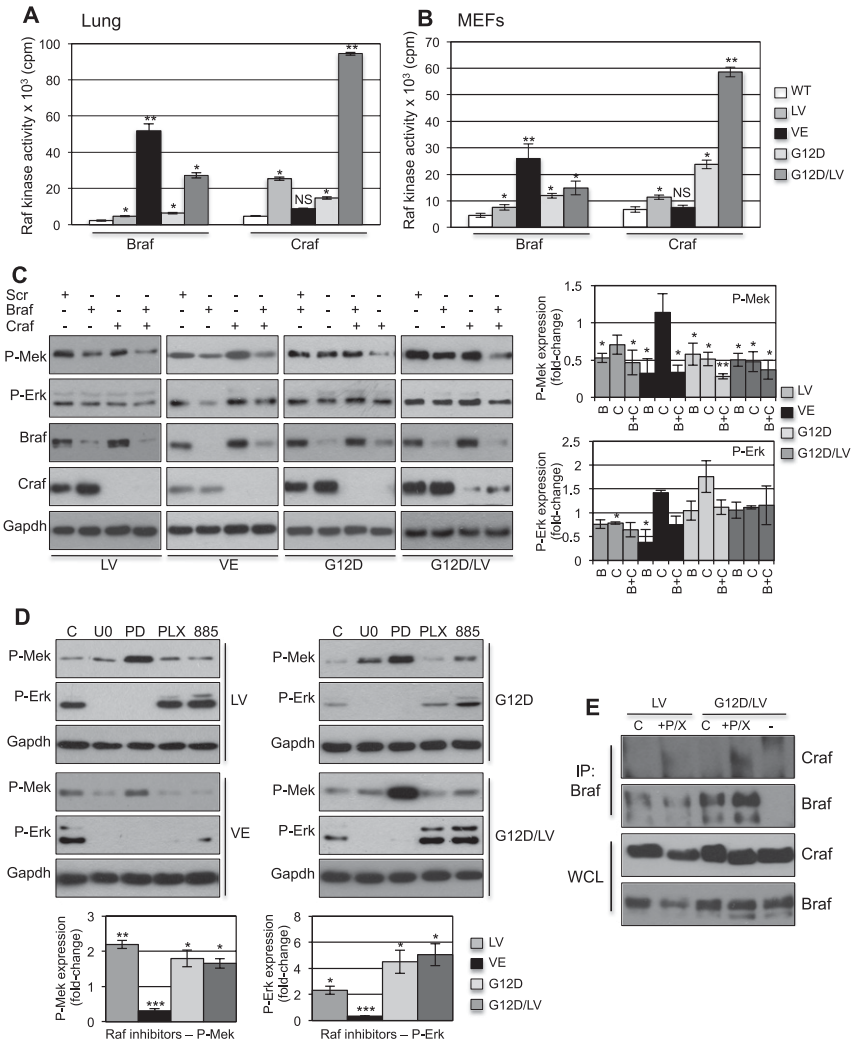

Figure 7. ^{L597V}Braf signals through Craf and Braf. (*A*) Raf kinase assays of protein lysates isolated from the lungs of *Braf*$^{+/+}$ (wild-type), *Braf*$^{+/LSL\text{-}V600E}$ (VE), *Kras*$^{+/Lox\text{-}G12D}$ (G12D), and *Braf*$^{+/LSL\text{-}L597V}$;*Kras*$^{+/LSL\text{-}G12D}$ (G12D/LV) mice treated with 1×10^8 pfu of AdCre 8 wk post-infection as well as protein lysates from lungs of *Braf*$^{+/LSL\text{-}L597V}$; CMV-*Cre*$^{+/o}$ (LV) mice. The mean of three samples is shown, and error bars represent the SD. (*B*) Raf kinase assays of protein lysates isolated from primary MEFs following 72 h post-AdCre treatment. The mean of three samples is shown, and error bars represent the SEM. (*A*,*B*) Student's *t*-test in comparison with respective Braf/Craf kinase activities for wild-type samples; (*) $P < 0.01$; (**) $P < 0.005$; (NS) not significant. (*C*) Immortalized MEFs of each genotype were transfected with scrambled (Scr) siRNA or *Craf*, *Braf*, or both siRNAs, and Western blots were analyzed with the antibodies indicated. Quantification of Mek/Erk phosphorylation following siRNA treatment is shown in the graphs on the *right*. P-Mek and P-Erk levels were normalized to Erk2, and the fold changes compared with Scr-treated samples are shown, where error bars indicate the SEM. Data were pooled from three experiments. (*D*) Immortalized MEFs of each genotype were treated with carrier (C), U0126 (U0), PD184352 (PD), PLX4720 (PLX), or SB590885 (885) for 4 h, and Western blots were analyzed with the antibodies indicated. Quantification of Mek/Erk phosphorylation following RAF inhibitor treatment is shown in the graphs *below*. P-Mek and P-Erk levels were normalized to Erk2, and the fold changes compared with carrier-treated samples are shown, where error bars indicate the SEM. Data were pooled from six samples, representing three different cell lines of each genotype treated with PLX4720 or SB590885. For Western blot quantitations in *C* and *D*, *P*-values were calculated using the Student's *t*-test; (*) $P < 0.01$; (**) $P < 0.005$; (***) $P < 0.001$. (*E*) Craf:Braf heterodimer formation. LV and G12D/LV MEFs were treated with either PD184352/PLX4720 (P/X) or carrier control (C), protein lysates were harvested and immunoprecipitated for Braf, and immunoprecipitates were analyzed for Braf and Craf. As a control, the G12D/LV samples were also immunoprecipitated without (–) primary antibody and analyzed with the same antibodies.

2011), and MEK inhibitors have proven effective at ameliorating disease phenotypes in RASopathy models (Schuhmacher et al. 2008; Anastasaki et al. 2009). Human cancer and RASopathy cell lines with the *^{L597V}BRAF* mutation are not currently available, and so we analyzed BRAF/MEK inhibitor responses using mouse cells. Each of the immortalized LV, VE, G12D, and G12D/LV MEFs was treated with either MEK inhibitors (U0126 and PD184352) or two ATP competitive RAF inhibitors (PLX4720 and SB590885). Mek/Erk activity was blocked in all cell lines in response to the MEK inhibitors (Fig. 7D). RAF inhibitors significantly suppressed Mek/Erk phosphorylations in the VE cells, as expected, but Mek/Erk phosphorylations were significantly induced in the LV, G12D, and G12D/LV cells (Fig. 7D). Like ^{WT}BRAF, ^{L597V}BRAF formed a heterodimer with CRAF in HEK293^{T} cells following transient transfection (Supplemental Fig. S7), and furthermore, heterodimer formation between endogenous Braf and Craf was strongly induced in LV and G12D/LV MEFs following dual treatment of these cells with PLX4720 and PD184352 (Fig. 7E).

Discussion

The *^{L597V}BRAF* mutation is a relatively unique mutation because it is acquired somatically in cancer samples yet is also mutated in RASopathy conditions. Here we identified the molecular basis for the involvement of the mutation in these two pathologies. Using a knock-in mouse model, we show that ^{L597V}Braf can induce weak activation of the Mek/Erk pathway and that this is sufficient to drive RASopathy hallmarks but not cancer. ^{L597V}Braf only contributes to cancer when it is coexpressed with another oncogenic mutation, and in this study we demonstrate a modifying effect on ^{G12D}Kras-driven oncogenesis. We also found that RAF inhibitors induce paradoxical activation of the Mek/Erk pathway in ^{L597V}Braf mutant cells, cautioning against the use of vemurafenib/PLX4032 or other similar RAF inhibitors in the treatment of RASopathies or cancers carrying the mutation.

^{L597V}BRAF is the best-characterized mutation affecting residue L597. Previous studies have shown that it has intermediate kinase activity when overexpressed in COS cells (Wan et al. 2004), and, using endogenous expression from one allele of *Braf*, we confirmed the intermediate nature of ^{L597V}Braf and its weak impact on the Mek/Erk pathway (Fig. 2). The fact that RASopathy hallmarks can be induced by ^{L597V}Braf but not cancer suggests that activation of downstream signaling pathways, particularly the Mek/Erk pathway, needs to pass a key threshold for transformation to occur. *^{L597V}BRAF*—and presumably other *BRAF* mutations present in RASopathies—clearly cannot activate downstream pathways past this point. For cancer, acquisition of a second mutation is a requirement for tipping the balance, and this may explain why *^{L597}BRAF* mutations are coincident with other low MEK/ERK-activating mutants such as *^{S259A}CRAF* in occasional human cancers in addition to driver oncogenes with higher activity toward the MEK/ERK pathway (http://www.sanger.ac.uk/perl/genetics/CGP/cosmic). *BRAF* mutant human RASopathy patients (Sarkozy et al. 2009; Tidyman and Rauen 2009) and ^{L597V}Braf-expressing mice show some predisposition to cancer when aged (Supplemental Table S1); such lesions may arise as a result of "second hits" being acquired in genes that allow the transforming threshold to be surpassed.

It has been estimated that only seven to 15 somatic mutations in key "driver" genes are absolutely required for tumor development (Beerenwinkel et al. 2007), with the remainder being "passenger" mutations or bystanders that do not contribute to the carcinogenesis process. However, this is likely to be a gross oversimplification, since it does not account for the existence of genetic interactions that can modify drivers through epistatic mechanisms (Ashworth et al. 2011). While it is difficult to functionally prove the existence of such modifiers in human cancers, recent data from a transposon screen for genes involved in promoting *Apc*-driven intestinal tumorigenesis identified modifiers of the canonical Wnt pathway (March et al. 2011). We also previously described a functional interaction between the impaired-activity *^{D594A}Braf* mutation and oncogenic *Kras* in the induction of rapid onset melanoma in mice (Heidorn et al. 2010; Kamata et al. 2010). In this study, we characterized the intermediate-activity Braf mutant ^{L597V}Braf and found that it falls into the category of "epistatic modifier," as it does not act as an oncogenic driver by itself but is able to interact with ^{G12D}Kras to induce high levels of signaling through the Mapk pathway as well as through Mapk-independent pathways.

^{L597V}Braf induces a shift from AAH to adenoma lesions in the ^{G12D}Kras mutant lung (Fig. 5). Since adenomas are thought to arise through increased proliferation of AAH followed by the induction of senescence (Kerr 2001; Dankort et al. 2007), these data suggest that ^{L597V}Braf enhances the proliferation/senescence of ^{G12D}Kras mutant alveolar type II pneumocytes in vivo. Similarly, morphological transformation and growth of ^{G12D}Kras MEFs are more similar to that driven by ^{V600E}Braf when coexpressed with ^{L597V}Braf (Fig. 4). All in all, ^{L597V}Braf induces a partial transition from a ^{G12D}Kras mutant phenotype to a more ^{V600E}Braf-like phenotype, as confirmed at the molecular level by microarray analysis (Fig. 6). This is thought to be partly attributable to increased signaling through the Mek/Erk pathway, as together, ^{L597V}Braf and ^{G12D}Kras raise Mek/Erk activity levels to those similar to ^{V600E}Braf. In spite of this, the consequences for tumor development in the lung are somewhat paradoxical, as although enhanced adenoma formation is observed in the ^{L597V}Braf;^{G12D}Kras mutant lung compared with the ^{G12D}Kras mutant lung (Fig. 5A), as with the ^{V600E}Braf mutant lung, there is reduced adenocarcinoma progression. Thus, the selective drive for the evolution of human cancers with both the *^{L597V}BRAF* and *^{G12D}KRAS* mutations must occur in the initiation stage, regardless of the consequences for subsequent cancer progression.

In addition to a transition to a more ^{V600E}Braf-like molecular profile, ^{L597V}Braf together with ^{G12D}Kras induce

the expression of several genes that are not shared by ^{V600E}Braf or ^{G12D}Kras alone (Fig. 6D), suggesting the activation of Mek/Erk-independent and/or Ras-independent signaling pathways. This observation may be related to the fact that Craf is strongly activated in the double-mutant cells but is weakly activated in the ^{G12D}Kras cells and is low in the ^{V600E}Braf cells (Fig. 7A,B). Craf is known to operate through a number of Mek/Erk-independent signaling pathways (Niault et al. 2009), and conceivably, activation of these pathways may account for the unique sets of genes induced by ^{L597V}Braf combined with ^{G12D}Kras, although Craf has not previously been connected with genes involved in translation or RNA processing, which seem to be particularly enriched in this data set (Supplemental Table S4). Craf activity is also weakly elevated in the ^{L597V}Braf-expressing single-mutant MEFs, but these cells show a phenotype different from our previous analysis of MEFs expressing the impaired activity mutant ^{D594A}Braf (Kamata et al. 2010). Craf transactivation in this situation was shown to lead to immortalization of MEFs associated with induction of aneuploidy, and this was reversed by Craf inhibition. The reason for the difference between the two may be related to the fact that Craf is more strongly activated by the *^{D594A}Braf* mutation (approximately fivefold greater than wild-type MEFs) than the *^{L597V}Braf* mutation (~1.7-fold greater than wild-type MEFs). Alternatively, we have not yet ruled out a role of suppressed Braf activity in contributing to the evolution of aneuploidy in ^{D594A}Braf-expressing cells.

Throughout this study, we found that there was a good correlation between Raf activity and levels of Mek phosphorylation, but Erk phosphorylation was more variable. As demonstrated in other studies (Pratilas et al. 2009), this is related to the expression of Dusp6 and Sprouty2, negative regulators of the Mek/Erk pathway. Both are transcriptional targets of the pathway (Packer et al. 2009; Pratilas et al. 2009), and Sprouty2 has been shown to act as a tumor suppressor at least in the context of ^{G12D}Kras-mediated lung tumorigenesis (Shaw et al. 2007). Dusp6 is a dual-specificity phosphatase that acts downstream from Mek to inactivate Erk (Keyse 2008), whereas Sprouty2 acts at multiple levels of the Erk pathway, one way being through direct interaction with Raf (Kim and Bar-Sagi 2004). In MEFs and the lung, ^{V600E}Braf expression was found to induce very high levels of expression of these proteins (Figs. 2, 3), whereas ^{L597V}Braf did not at all, indicating higher Erk pathway output by ^{V600E}Braf and no feedback inhibition in the ^{L597V}Braf cells. Although levels of phospho-Mek were significantly higher in the ^{V600E}Braf mutant cells, phospho-Erk levels were similar in the two. This suggests that the pathway is sensitive to feedback inhibition below Mek at the level of Erk in the ^{V600E}Braf mutant cells, presumably through the action of Dusps, but insensitive to feedback inhibition upstream of Mek. The mechanism of insensitivity upstream of Mek may be related to the fact that the active Braf kinase conformation of ^{V600E}Braf cannot bind to Sprouty2 (Brady et al. 2009). Regardless of the mechanism, feedback regulation of the Erk pathway offers exquisite control of the pathway and is important in regulation of the ultimate biological outputs of the pathway.

Using siRNA, we show that ^{L597V}Braf activates the Mek/Erk pathway through its intrinsic Braf kinase activity as well as through transactivation of Craf on both the ^{WT}Kras and ^{G12D}Kras backgrounds (Fig. 7C). This is a scenario similar to ^{G12D}Kras cells expressing ^{WT}Braf and ^{WT}Craf (Blasco et al. 2011; Karreth et al. 2011) but different from cells expressing ^{V600E}Braf that signal entirely through its intrinsic activity. As with ^{WT}Braf, the likely mechanism for Craf transactivation by ^{L597V}Braf is through dimerization, membrane localization, and interaction with Ras.GTP. Given this observation, it is not surprising that ATP-competitive RAF inhibitors (PLX4720 and SB590885) activate the Mek/Erk pathway in ^{L597V}Braf mutant cells (Fig. 7D). This finding has important clinical implications, since it suggests that response to vemurafenib (PLX4032) is dependent on not just whether a tumor has a *^{WT}BRAF* or *^{V600E}BRAF* allele, but also the type of *BRAF* mutation and the level of mutant BRAF kinase activity acquired. Mutants such as ^{V600E}BRAF with activity approximately eightfold greater than ^{WT}BRAF clearly allow response to vemurafenib, but mutants with approximately twofold greater activity, such as ^{L597V}BRAF, do not. It will be interesting to assess what threshold of BRAF activity is required to allow response to vemurafenib, and related to this is the question of whether mutant BRAF isoforms undergo dimerization and the levels of RAS activation achieved in cells with different levels of BRAF activity.

Materials and methods

Mouse strains and genotyping

All animal experiments were carried out under U.K. Home Office License authority. *Braf$^{+/LSL\text{-}L597V}$* mice were generated in the same way as *Braf$^{+/LSL\text{-}V600E}$* (Mercer et al. 2005) and *Braf$^{+/LSL\text{-}D594A}$* (Heidorn et al. 2010; Kamata et al. 2010) mice, except *Braf* exon 15 contained the C1789A mutation. The *Kras$^{+/LSL\text{-}G12D}$* mice were as previously reported (Jackson et al. 2001) and were obtained from the Mouse Models of Human Cancers Consortium (MMHCC) Mouse Repository (http://www.nih.gov/science/models/mouse/resources/mmhcc.html). All strains were maintained by backcrossing onto the C57BL6J background, and phenotype analysis was performed for mice that had been maintained for more than five generations on this background strain. Genotyping of *Braf$^{+/LSL\text{-}L597V}$*, *Braf$^{+/LSL\text{-}V600E}$*, *Braf$^{+/Lox\text{-}L597V}$*, *Braf$^{+/Lox\text{-}V600E}$*, and *Cre* alleles was performed using the primer systems previously reported (Mercer et al. 2005). The *Kras$^{LSL\text{-}G12D}$* allele was genotyped using primers 5′-AGCTAGCCACCATGGCTTGAGTAAGTCTGCA-3′ and 5′-CCTTTACAAGCGCACGCAGATGTAGA-3′. To monitor Cre recombination, the *Kras$^{Lox\text{-}G12D}$* allele was genotyped with primers 5′-TGACACCAGCTTCGGCTTCCT-3′ and 5′-TCCGAATTCAGTGACTACAGATGTACAGA-3′. Infection of lungs with AdCre (University of Iowa) was performed as described (Jackson et al. 2001; Dankort et al. 2007).

Histology and tissue staining

Tissues were processed for histology and stained as described (Mercer et al. 2005). For cardiomyocyte analysis, cell membranes were stained with FITC-conjugated wheat germ agglutinin (WGA) (Sigma). For quantification, H&E- and WGA-stained

sections were assessed using Image J software (http://rsbweb.nih.gov/ij).

Cells and treatments

MEFs were isolated as reported (Mercer et al. 2005) and maintained in DMEM with 10% FCS and penicillin/streptomycin. MEFs were infected with AdCre or Adβgal by addition of $\sim 1 \times 10^8$ plaque-forming units (pfu) directly to the culture medium. For growth assays, cells were plated at a density of 3×10^4 in triplicate and recounted every 2 d for 8 d. For immortalization assays, MEFs were plated at 3×10^5 cells per 6-cm plate in triplicate, counted, and replated every 3 d. For *Braf* and *Craf* siRNA, ON-TARGETplus SMARTpool siRNAs (Dharmacon) were used and transfected using Lipofectamine 2000 as previously described (Noble et al. 2008). For inhibitor treatments, MEFs at ~80% confluency were treated with 10 μM U0126, 1 μM PD184352, 0.3 μM PLX4720, or 1 μM SB590885 for 4 h or a volume of DMSO equivalent as the carrier control.

Immunoblotting and kinase assays

Protein lysates were prepared by previously published methods (Huser et al. 2001; Mercer et al. 2005). The antibodies used were as follows: phospho-Erk1/2 (Cell Signaling Technologies, #9101S), Erk2 (Santa Cruz Biotechnology, #SC-1647), Craf (BD Biosciences, #610153), phospho-Mek1/2 (Cell Signaling Technologies, #9154S), Gapdh (Millipore, #MAB374), Sprouty2 (Abcam, #AB50317), Dusp6 (Abcam, #AB76310), and Braf (Santa Cruz Biotechnology, #SC-5284). Raf kinase activity was measured as described (Huser et al. 2001; Wan et al. 2004), and the primary antibodies used for immunoprecipitation were Braf (as above) and Craf (Santa Cruz Biotechnology, SC-133). Western blots were quantitated using ImageJ software.

RNA extraction, labeling, and microarray processing

RNA from three biological replicates of immortalized MEFs of each genotype was prepared using a Qiagen RNeasy kit according to the manufacturer's recommendations and quality was assessed using a Bioanalyser 2100 (Agilent). RNA labeling and hybridization to Affymetrix GeneChip Mouse Gene 1.0ST arrays were performed by standard protocols (http://www.gladstone.ucsf.edu/gladstone/site/genomicscore/section/380).

Bioinformatic analysis

Microarrays were normalized for array-specific effects using Affymetrix's Robust Multi-Array (RMA) normalization. Normalized array values were reported on a $\log_2$ scale. For statistical analyses, all array probe sets where no experimental groups had an average $\log_2$ intensity of >3.0 were removed. Linear models were fitted for each gene using the Bioconductor limma package in R (Gentleman et al. 2004; Smyth 2004). Moderated *t*-statistics, fold change, and the associated *P*-values were calculated for each gene. To account for the fact that thousands of genes were tested, FDR-adjusted values were calculated using the Benjamini-Hochberg method (Benjamini and Hochberg 1995).

Acknowledgments

We thank Linda Yee for providing microarray support, Kees Straatman for help with image analysis, and Biomedical Services at Leicester for their invaluable contribution. This work was funded by a Cancer Research UK program grant (C1362/A6969) and Royal Society Wolfson Merit Award to C.A.P.

References

Anastasaki C, Estep AL, Marais R, Rauen KA, Patton EE. 2009. Kinase-activating and kinase-impaired cardio–facio–cutaneous syndrome alleles have activity during zebrafish development and are sensitive to small molecule inhibitors. *Hum Mol Genet* **18:** 2543–2554.

Ashworth A, Lord CJ, Reis-Filho JS. 2011. Genetic interactions in cancer progression and treatment. *Cell* **145:** 30–38.

Basso AD, Kirschmeier P, Bishop WR. 2006. Lipid posttranslational modifications. Farnesyl transferase inhibitors. *J Lipid Res* **47:** 15–31.

Beerenwinkel N, Antal T, Dingli D, Traulsen A, Kinzler KW, Velculescu VE, Vogelstein B, Nowak MA. 2007. Genetic progression and the waiting time to cancer. *PLoS Comput Biol* **3:** e225. doi: 10.1371/journal.pcbi.0030225.

Benjamini Y, Hochberg Y. 1995. Controlling the false discovery rate: A practical and powerful approach to multiple testing. *J R Stat Soc Ser B Methodol* **57:** 289–300.

Blasco RB, Francoz S, Santamaria D, Canamero M, Dubus P, Charron J, Baccarini M, Barbacid M. 2011. c-Raf, but not B-Raf, is essential for development of K-Ras oncogene-driven non-small cell lung carcinoma. *Cancer Cell* **19:** 652–663.

Brady SC, Coleman ML, Munro J, Feller SM, Morrice NA, Olson MF. 2009. Sprouty2 association with B-Raf is regulated by phosphorylation and kinase conformation. *Cancer Res* **69:** 6773–6781.

Champion KJ, Bunag C, Estep AL, Jones JR, Bolt CH, Rogers RC, Rauen KA, Everman DB. 2011. Germline mutation in BRAF codon 600 is compatible with human development: De novo p.V600G mutation identified in a patient with CFC syndrome. *Clin Genet* **79:** 468–474.

Chapman PB, Hauschild A, Robert C, Haanen JB, Ascierto P, Larkin J, Dummer R, Garbe C, Testori A, Maio M, et al. 2011. Improved survival with vemurafenib in melanoma with BRAF V600E mutation. *N Engl J Med* **364:** 2507–2516.

Dankort D, Filenova E, Collado M, Serrano M, Jones K, McMahon M. 2007. A new mouse model to explore the initiation, progression, and therapy of BRAFV600E-induced lung tumors. *Genes Dev* **21:** 379–384.

Davies H, Bignell GR, Cox C, Stephens P, Edkins S, Clegg S, Teague J, Woffendin H, Garnett MJ, Bottomley W, et al. 2002. Mutations of the BRAF gene in human cancer. *Nature* **417:** 949–954.

Dumaz N, Hayward R, Martin J, Ogilvie L, Hedley D, Curtin JA, Bastian BC, Springer C, Marais R. 2006. In melanoma, RAS mutations are accompanied by switching signaling from BRAF to CRAF and disrupted cyclic AMP signaling. *Cancer Res* **66:** 9483–9491.

Ehrenreiter K, Kern F, Velamoor V, Meissl K, Galabova-Kovacs G, Sibilia M, Baccarini M. 2009. Raf-1 addiction in Ras-induced skin carcinogenesis. *Cancer Cell* **16:** 149–160.

Engelman JA, Chen L, Tan X, Crosby K, Guimaraes AR, Upadhyay R, Maira M, McNamara K, Perera SA, Song Y, et al. 2008. Effective use of PI3K and MEK inhibitors to treat mutant Kras G12D and PIK3CA H1047R murine lung cancers. *Nat Med* **14:** 1351–1356.

Gentleman RC, Carey VJ, Bates DM, Bolstad B, Dettling M, Dudoit S, Ellis B, Gautier L, Ge Y, Gentry J, et al. 2004. Bioconductor: Open software development for computational biology and bioinformatics. *Genome Biol* **5:** R80. doi: 10.1186/gb-2004-5-10-r80.

Hatzivassiliou G, Song K, Yen I, Brandhuber BJ, Anderson DJ, Alvarado R, Ludlam MJ, Stokoe D, Gloor SL, Vigers G, et al. 2010. RAF inhibitors prime wild-type RAF to activate the MAPK pathway and enhance growth. *Nature* **464:** 431–435.

Heidorn SJ, Milagre C, Whittaker S, Nourry A, Niculescu-Duvas I, Dhomen N, Hussain J, Reis-Filho JS, Springer CJ, Pritchard C, et al. 2010. Kinase-dead BRAF and oncogenic RAS cooperate to drive tumor progression through CRAF. *Cell* **140:** 209–221.

Huser M, Luckett J, Chiloeches A, Mercer K, Iwobi M, Giblett S, Sun XM, Brown J, Marais R, Pritchard C. 2001. MEK kinase activity is not necessary for Raf-1 function. *EMBO J* **20:** 1940–1951.

Jackson EL, Willis N, Mercer K, Bronson RT, Crowley D, Montoya R, Jacks T, Tuveson DA. 2001. Analysis of lung tumor initiation and progression using conditional expression of oncogenic K-ras. *Genes Dev* **15:** 3243–3248.

Ji H, Wang Z, Perera SA, Li D, Liang MC, Zaghlul S, McNamara K, Chen L, Albert M, Sun Y, et al. 2007. Mutations in BRAF and KRAS converge on activation of the mitogen-activated protein kinase pathway in lung cancer mouse models. *Cancer Res* **67:** 4933–4939.

Johannessen CM, Boehm JS, Kim SY, Thomas SR, Wardwell L, Johnson LA, Emery CM, Stransky N, Cogdill AP, Barretina J, et al. 2010. COT drives resistance to RAF inhibition through MAP kinase pathway reactivation. *Nature* **468:** 968–972.

Kamata T, Hussain J, Giblett S, Hayward R, Marais R, Pritchard C. 2010. BRAF inactivation drives aneuploidy by deregulating CRAF. *Cancer Res* **70:** 8475–8486.

Karasarides M, Chiloeches A, Hayward R, Niculescu-Duvaz D, Scanlon I, Friedlos F, Ogilvie L, Hedley D, Martin J, Marshall CJ, et al. 2004. B-RAF is a therapeutic target in melanoma. *Oncogene* **23:** 6292–6298.

Karreth FA, Frese KK, Denicola GM, Baccarini M, Tuveson DA. 2011. C-Raf is required for the initiation of lung cancer by K-Ras. *Cancer Discov* **1:** 128–136.

Kerr KM. 2001. Pulmonary preinvasive neoplasia. *J Clin Pathol* **54:** 257–271.

Keyse SM. 2008. Dual-specificity MAP kinase phosphatases (MKPs) and cancer. *Cancer Metastasis Rev* **27:** 253–261.

Kim HJ, Bar-Sagi D. 2004. Modulation of signalling by Sprouty: A developing story. *Nat Rev Mol Cell Biol* **5:** 441–450.

Malumbres M, Barbacid M. 2003. RAS oncogenes: The first 30 years. *Nat Rev Cancer* **3:** 459–465.

March HN, Rust AG, Wright NA, Ten Hoeve J, de Ridder J, Eldridge M, van der Weyden L, Berns A, Gadiot J, Uren A, et al. 2011. Insertional mutagenesis identifies multiple networks of cooperating genes driving intestinal tumorigenesis. *Nat Genet* **43:** 1202–1209.

Mercer K, Giblett S, Green S, Lloyd D, DaRocha Dias S, Plumb M, Marais R, Pritchard C. 2005. Expression of endogenous oncogenic V600EB-raf induces proliferation and developmental defects in mice and transformation of primary fibroblasts. *Cancer Res* **65:** 11493–11500.

Montagut C, Settleman J. 2009. Targeting the RAF–MEK–ERK pathway in cancer therapy. *Cancer Lett* **283:** 125–134.

Nazarian R, Shi H, Wang Q, Kong X, Koya RC, Lee H, Chen Z, Lee MK, Attar N, Sazegar H, et al. 2010. Melanomas acquire resistance to B-RAF(V600E) inhibition by RTK or N-RAS upregulation. *Nature* **468:** 973–977.

Niault T, Sobczak I, Meissl K, Weitsman G, Piazzolla D, Maurer G, Kern F, Ehrenreiter K, Hamerl M, Moarefi I, et al. 2009. From autoinhibition to inhibition in *trans*: The Raf-1 regulatory domain inhibits Rok-α kinase activity. *J Cell Biol* **187:** 335–342.

Noble C, Mercer K, Hussain J, Carragher L, Giblett S, Hayward R, Patterson C, Marais R, Pritchard CA. 2008. CRAF autophosphorylation of serine 621 is required to prevent its proteasome-mediated degradation. *Mol Cell* **31:** 862–872.

Packer LM, East P, Reis-Filho JS, Marais R. 2009. Identification of direct transcriptional targets of (V600E)BRAF/MEK signalling in melanoma. *Pigment Cell Melanoma Res* **22:** 785–798.

Pearson G, Robinson F, Beers Gibson T, Xu BE, Karandikar M, Berman K, Cobb MH. 2001. Mitogen-activated protein (MAP) kinase pathways: Regulation and physiological functions. *Endocr Rev* **22:** 153–183.

Pierpont EI, Pierpont ME, Mendelsohn NJ, Roberts AE, Tworog-Dube E, Rauen KA, Seidenberg MS. 2010. Effects of germline mutations in the Ras/MAPK signaling pathway on adaptive behavior: Cardiofaciocutaneous syndrome and Noonan syndrome. *Am J Med Genet A* **152A:** 591–600.

Poulikakos PI, Zhang C, Bollag G, Shokat KM, Rosen N. 2010. RAF inhibitors transactivate RAF dimers and ERK signalling in cells with wild-type BRAF. *Nature* **464:** 427–430.

Pratilas CA, Taylor BS, Ye Q, Viale A, Sander C, Solit DB, Rosen N. 2009. (V600E)BRAF is associated with disabled feedback inhibition of RAF–MEK signaling and elevated transcriptional output of the pathway. *Proc Natl Acad Sci* **106:** 4519–4524.

Rauen KA, Banerjee A, Bishop WR, Lauchle JO, McCormick F, McMahon M, Melese T, Munster PN, Nadaf S, Packer RJ, et al. 2011. Costello and cardio–facio–cutaneous syndromes: Moving toward clinical trials in RASopathies. *Am J Med Genet C Semin Med Genet* **157:** 136–146.

Rodriguez-Viciana P, Tetsu O, Tidyman WE, Estep AL, Conger BA, Cruz MS, McCormick F, Rauen KA. 2006. Germline mutations in genes within the MAPK pathway cause cardio–facio–cutaneous syndrome. *Science* **311:** 1287–1290.

Sarkozy A, Carta C, Moretti S, Zampino G, Digilio MC, Pantaleoni F, Scioletti AP, Esposito G, Cordeddu V, Lepri F, et al. 2009. Germline BRAF mutations in Noonan, LEOPARD, and cardiofaciocutaneous syndromes: Molecular diversity and associated phenotypic spectrum. *Hum Mutat* **30:** 695–702.

Schuhmacher AJ, Guerra C, Sauzeau V, Canamero M, Bustelo XR, Barbacid M. 2008. A mouse model for Costello syndrome reveals an Ang II-mediated hypertensive condition. *J Clin Invest* **118:** 2169–2179.

Schwenk F, Baron U, Rajewsky K. 1995. A cre-transgenic mouse strain for the ubiquitous deletion of loxP-flanked gene segments including deletion in germ cells. *Nucleic Acids Res* **23:** 5080–5081.

Shaw AT, Meissner A, Dowdle JA, Crowley D, Magendantz M, Ouyang C, Parisi T, Rajagopal J, Blank LJ, Bronson RT, et al. 2007. Sprouty-2 regulates oncogenic K-ras in lung development and tumorigenesis. *Genes Dev* **21:** 694–707.

Smyth GK. 2004. Linear models and empirical bayes methods for assessing differential expression in microarray experiments. *Stat Appl Genet Mol Biol* **3:** Article3. doi: 10.2202/1544-6115.1027.

Su F, Viros A, Milagre C, Trunzer K, Bollag G, Spleiss O, Reis-Filho JS, Kong X, Koya RC, Flaherty KT, et al. 2012. RAS mutations in cutaneous squamous-cell carcinomas in patients treated with BRAF inhibitors. *N Engl J Med* **366:** 207–215.

Tidyman WE, Rauen KA. 2009. The RASopathies: Developmental syndromes of Ras/MAPK pathway dysregulation. *Curr Opin Genet Dev* **19:** 230–236.

Tuveson DA, Shaw AT, Willis NA, Silver DP, Jackson EL, Chang S, Mercer KL, Grochow R, Hock H, Crowley D, et al. 2004. Endogenous oncogenic K-ras(G12D) stimulates proliferation and widespread neoplastic and developmental defects. *Cancer Cell* **5:** 375–387.

Wan PT, Garnett MJ, Roe SM, Lee S, Niculescu-Duvaz D, Good VM, Jones CM, Marshall CJ, Springer CJ, Barford D, et al. 2004. Mechanism of activation of the RAF–ERK signaling pathway by oncogenic mutations of B-RAF. *Cell* **116:** 855–867.